ELSEVIER

Experimental Thermal and Fluid Science 17 (1998) 238–247

Experimental Thermal and Fluid Science

Local convective heat transfer from a vertical flat surface to oblique submerged impinging jets of large Prandtl number liquid

C.F. Ma [a,*], Q. Zheng [a], H. Sun [a], K. Wu [a], K. Horii [b]

[a] *Department of Thermal Science and Engineering, Beijing Polytechnic University, Beijing 100022, People's Republic of China*
[b] *Shirayuri College, Tokyo 182, Japan*

Accepted 9 September 1997

Abstract

An experimental study has been carried out to investigate the effect of the jet inclination on convective heat transfer from vertical heaters to circular submerged liquid jets. Local heat transfer measurements were made with obliquely impinging circular jets of transformer oil issued from both pipe-type and orifice-type nozzles in the range of jet Reynolds number from 162 to 958, corresponding to the jet velocity from 1.73 to 19.1 m/s. Variations both of the location and the magnitude of maximum heat transfer rates were determined and correlated in the range of jet inclination angles from 90° to 45°. Profiles of local heat transfer coefficients were obtained both along the *x*- and *y*- axes. A correlation was presented to predict the radial distribution of local Nusselt number in the *x*-axis. Comparison was made of the present results with those from available literature related to oblique circular liquid and air jets.

Keywords: Jets; Forced convection; Larger Prandtl number liquid

1. Introduction

Single and multiple impinging jets of gas or liquid are encountered commonly in many technical processes because of their excellent heat/mass transfer performance. Impingement heat transfer with air jets has been extensively investigated. Comprehensive reviews on this topic have been presented by Martin [1], Downs and James [2] and Hrycak [3]. Recently, increased attention has been directed to applications of liquid jets as the heat transfer coefficient can be increased several orders of magnitude in comparison with that of gas jets [4,5]. As an attractive means of providing very high heat/mass transfer rates, liquid jet impingement has been employed in cooling systems of heat engines [6] or electronic devices [7–12] and thermal treatment of metals [13,14]. With liquid as working fluid, two operation modes are possible: submerged jet and free-surface jet. In the former case, a liquid jet is discharged into the same liquid. In the latter, a liquid jet is exposed to a gaseous environment.

A vast amount of literature exists on heat transfer with impinging jets. Almost all the research efforts were devoted to the study of normal impingement heat transfer. In engineering practice, influenced by spent flows from other jets the impinging jets may strike on the target surfaces at oblique angles even if leaving the nozzles in the direction perpendicular to the surfaces. In many applications, the device designers have to choose oblique impingement scheme due to constraints on the arranging of the jet nozzles or due to the special shape of the heat transfer surfaces. Consequently, detailed knowledge is required of the effect of the jet inclination on the impingement heat transfer. However, the available information on jet impingement heat transfer is mainly restricted to perpendicularly impinging jets. Studies of heat transfer with oblique jets are relatively rare, particularly with liquid jets. Quasi-local heat transfer measurements were made by Perry [15] with oblique round air jets. Using a mass transfer technique, Sparrow and Lovell [16] measured local mass transfer coefficient with oblique impinging round air jets over the range of Reynolds number from 2500 to 10 000. For circular jets they first reported the displacement of the point maximum mass transfer from the geometrical impingement point. Local heat transfer was systematically studied by Goldstein and Franchett [17] with oblique circular impinging air jets utilizing a liquid crystal technique in the range of Reynolds number between 10 000 and 35 000. With

* Corresponding author. Tel.: +86 10 6739-1985; fax: +86 10 6618-6314; e-mail: machf@solaris.bjpu.edn.cn.

0894-1777/98/$19.00
PII: S0894-1777(97)10040-1

regard to liquid jets, the influence of jet inclination was studied by Stevens and Webb [18] with circular water jets and Ma et al. [19] with circular oil jets, respectively. Both the two investigations are related with free-surface jets. To the best knowledge of the present authors, characteristics of impingement heat transfer with submerged oblique circular liquid jets have not been reported in open literature.

The objective of this study was to carry out an extensive investigation of the effect of jet inclination on impingement heat transfer for single circular submerged jets of transformer oil. The experiments were performed using both pipe-type and orifice-type nozzles (nominal size is 1 mm or 3 mm in diameter) in the range of jet Reynolds number from 162 to 958 with jet velocity up to 19 m/s. Local heat transfer measurements were made with jet inclination angle from 90° to 45°. The influence of nozzle configuration on local heat transfer was examined experimentally. Correlations were developed to predict both the local heat transfer profiles and the variations of the location and magnitude of the maximum heat transfer coefficients. Comparison of local heat transfer characteristics was made between submerged and free-surface liquid jets, as well as between the circular liquid and air jets. Based on the large body of local heat transfer data collected in this work, all the important aspects of jet inclination effect were carefully examined and clarified with single circular jets of large Prandtl number liquid. It is hoped that the results of the present study will improve our basic knowledge on heat transfer process with impinging liquid jets and provide useful information for developing impingement cooling schemes of internal combustion engines or electronic devices with liquid jets.

2. Experimental apparatus and method

2.1. Experimental apparatus

Transformer oil was chosen as the test liquid in this study. The test liquid was circulated in a closed loop which had provision for filtering, metering, preheating and cooling. The test chamber was constructed of stainless steel with three visual ports as shown in Fig. 1. The bottom section of the cover on the chamber was transparent. A flexible polyethylene tube joined the two sections of the cover. The test section assembly was vertically fixed on one side of the test chamber. The details of the test section are shown in Fig. 2. The main part was a strip of 10 μm thick constantan foil with a heated section of 10 mm × 5 mm (nominal) exposed to the coolant. The strip on either side of this active section was soldered to copper bus blocks, which were in turn connected to power leads. The heated section of the foil was cemented to a bakelite block inserted between copper blocks. The assembly was cemented in a Plexiglas disk fixed in brass housing with a screwed flange. The test section was highly insulated by fiberglass to minimize heat loss. The temperature of the center of the inner surface of the heater was measured with a 40 gage iron–constantan thermocouple which was electrically insulated from the heater yet in close thermal contact. The active section of the constantan foil was used as an electrically heating element as well as a heat transfer surface. AC power to the test section was provided by a 50 A power supply.

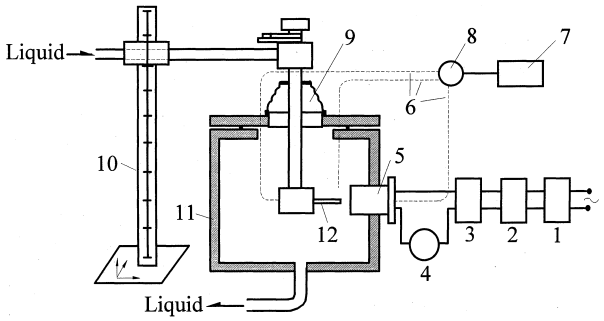

Fig. 1. Details of test chamber and instrumentation. 1, Stabilized power supply; 2, voltage regulator; 3, voltage transformer; 4, amperemeter; 5, test section assembly; 6, thermocouples; 7, MV meter; 8, switcher; 10, three-dimensional coordinate frame; 11, chamber; 12, jet tube.

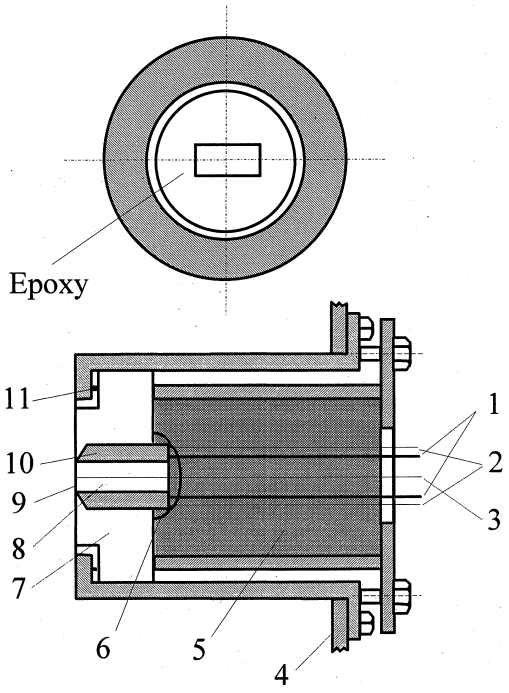

Fig. 2. Details of electrically heated test section. 1, Power lead; 2, voltage tap; 3, thermocouple; 4, tank wall; 5, fiberglass; 6, epoxy; 7, plexiglass; 8, bakelite; 9, 10 μ thick constantan foil; 10, copper block; 11, O-ring.

In most experiments oil jets issued from a horizontal jet tube of 0.987 mm inside diameter and 35 mm length. Using the large length-to-diameter ratio tube, a fully developed laminar pipe flow can be obtained at nozzle exit. For the measurements of displacement of maximum

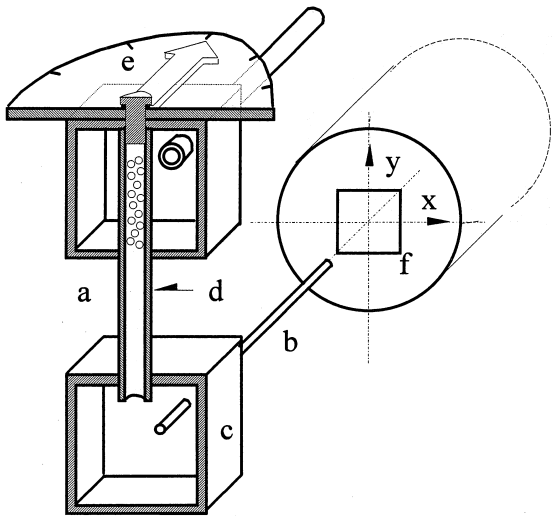

Fig. 3. Details of nozzle assembly.

heat transfer location a large size tube (3 mm nominal inside diameter) was used. As shown in Fig. 3, the oil was supplied from a vertical delivery tube (a) to the jet nozzle, (b) passing a plenum box of 125 cm^3, (c) Both the jet tube and the delivery tube were made of stainless steel and fixed with the plenum box. Their axes were perpendicular with each other in a vertical plane. The jet tube could be rotated in the horizontal plane about the axis of the delivery tube by pivoting the latter upon a pivot bearing (d). The inclination of the jet tube to the test section could be read by the angle markings scribed on the surface of a horizontal plate (e) with an estimated angular uncertainty of ±1°. The jet-tube-delivery assembly was fixed on a three-dimensional coordinate rack and could be adjusted with respect to the test section (f) with placements accomplished within ±0.01 mm. The jet temperature was measured with a 40 gage iron–constantan thermocouple placed inside the plenum box close to the entrance of the jet tube. The oil temperature in the test chamber was also monitored by a thermocouple of the same type. In order to study the effect of the nozzle geometry, experiments were also performed with an orifice-type nozzle that was a round hole of 0.99 mm diameter made in a plane plate of 3.0 mm thickness. Due to flexible nature of the plastic seal at the top of the chamber, the pressure in the chamber is considered close to the atmosphere.

2.2. Procedure and data reduction

The heat transfer surface was left in the original highly polished condition and cleaned with acetone before tests. The area of the heated surface was carefully measured for each test section assembly with a tool maker's microscope of 0.001 mm resolution. Heat flux was calculated from the electrical power supplied to the test section and the area of one side of the heated surface. It was determined by the following formula:

$$q = \frac{I^2 R}{A}, \tag{1}$$

where the resistance R was measured accurately with direct current before experiments. It was verified in preliminary tests that the variation of resistance with temperature could be neglected (less than ±0.1%), as the heater temperature variation was less than 50 K in the present study and the variation in resistivity with temperature is extremely small for constantan. The current intensity was measured by an amperemeter.

In preliminary experiments the jet tube was oriented normally to the test section. The distance between the nozzle and the target surface was accurately adjusted by means of the three-dimensional frame. In order to ensure that the nozzle centerline coincided with the center of the heater, a procedure of centering was developed whereby the jet was moved on the heated surface until minimum wall temperature was recorded by the thermocouple. In experiments with oblique jets, the jet inclination angle was fixed and the jet tube was adjusted again by the three-dimensional rack to warrant the coincidence of the center of the heater with the geometric intersection of the jet axis with the impingement plane at a fixed nozzle-to-plate spacing. The measured wall temperature at the heater center was taken as the local value. By recording this temperature for various locations of the jet tube, both horizontal (x-axis) and vertical (y-axis) temperature distributions could be obtained for given jet conditions and surface heat fluxes. Properties of the working fluid were evaluated at the film temperature by averaging the wall and jet static temperature. In the experiments the temperature of the jets and the oil in the container were accommodated with each other so that their difference could be less than 1 K for eliminating the effect of ambient fluid entrainment into the impinging jets on the heat transfer process. The heater wall temperature was sustained at about 10 K higher than the jet temperature. The local heat transfer coeffient was calculated from the heat flux and the local wall temperature

$$h = \frac{q}{T_w - T_{aw}}, \tag{2}$$

where the adiabatic wall temperature T_{aw} was determined by

$$T_{aw} = T_j + r\frac{u^2}{2C_p}, \tag{3}$$

where the velocity u was calculated from the measured flow rate and the nozzle area. The recovery factor can be obtained from Ref. [19]. During the experiment, the difference between T_j and T_{aw} was adjusted to be maintained approximately at 10 K.

2.3. Uncertainty of experimental results

The uncertainty in Nusselt number was influenced primarily by the determination of heat flux and wall temperature. The surface heat flux was affected by the variation of the constantan foil thickness that was

claimed in the suppliers specification to be less than ±3% of the normal value. This value is taken as the indicator of heat flux variation due to foil thickness nonuniformity. Preliminary experiments were performed to check heat loss from the heater, and indicated that with jet impingement the maximum conduction loss to the back of the heater assembly was less than 0.8% of the power input to the heater. This conclusion was supported by a conduction analysis for this study. So, no correction was included for such conduction loss in this work. The determination of the heater surface temperature was related to the thermal resistance of the adhesive layer between the thermocouple bead and the back side of the foil. During the manufacture process the foil was strongly suppressed to the top surface of the bakelite block to minimize the thickness of the adhesive layer in between. Measurements were made of the adhesive thickness with several used test sections after their failure in experiments. The thickness was determined between 0.04 and 0.1 mm. Taking the typical value of the thermal conductivity of adhesive as 0.29 W/m.k, the thermal resistance across the adhesive layer was estimated between 1.4×10^{-4} and 3.4×10^{-4} m^2kW^{-1}. As the conduction heat loss was less than 0.8% of the power input, and its main part passed through the bus bars, the uncertainty arising from positioning of the thermocouple bead was estimated to be always less than 0.15 K in this study. Another source of the uncertainty in wall temperature was concerned with lateral heat conduction along the constantan foil caused by the sharp radial variation of the heat transfer coefficient around the stagnation zone. Using the measured wall temperature distribution, this uncertainty was determined to be negligible (less than 0.8%) due to the extremely small thickness of the foil. All the thermocouples were calibrated to an accuracy of ±0.1 K before experiments. The uncertainty in Nusselt number was determined to be less than ±5%. The uncertainty in Reynolds number was affected by the measurement of the flowrate and the nozzle exit area. While the flowmeter was carefully calibrated, the nozzle exit area was precisely determined using the tool maker's microscope of 0.001 resolution. The uncertainty in Reynolds number did not exceed ±5.5%.

3. Experimental results and discussion

3.1. Displacement of maximum heat transfer point

Upstream displacement of maximum heat/mass transfer point is an important phenomena observed with oblique jet impingement. The displacement has been quantitatively determined both with submerged air jets [16,17] and free-surface liquid jets [18,19]. The displacement was measured in the present study with oil jets issuing from a jet tube of 3 mm diameter for four Reynolds numbers at a constant nozzle-to-plate spacing of $z/d = 4$. After normalization to the nozzle diameter, measured displacements are shown in Fig. 4. It is seen

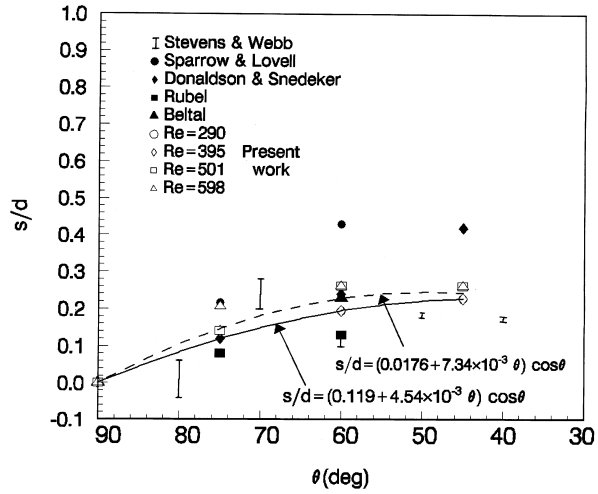

Fig. 4. Displacement distance between the maximum heat transfer point and the geometric stagnation point.

from the figure that the displacement increases monotonically with the increasing of jet inclination. It is also noted that the influence of jet Reynolds number on the displacement seems insignificant in the range of the present experimental parameters. An empirical equation was developed to correlate the measured displacements in the present work

$$s/d = (0.0176 + 0.00734\theta)\cos\theta, \quad (4)$$

where θ is expressed in radians. The correlation is compared with experimental data as shown in Fig. 5. In general, the agreement between the correlation and the data is quite good.

As the displacement of maximum heat transfer point for submerged liquid jets appears not to have been previously measured, the present results can be compared only with those associated with free-surface liquid jets. The correlation developed by Ma et al. [19] for free-surface oil jets and the data obtained by the Stevens and Webb for free-surface water jets are shown in Fig. 4 for comparison with the present results. The free-surface oil jet results [19] were measured by the present authors with the same experimental method and apparatus over a similar range of experimental parameters. It is found from the comparison that the displacement of submerged jets is slightly higher than that with free-surface jets. It may be attributed to the stronger entrainment and consequent pre-impingement spreading for submerged jets. The data reported by Stevens and Webb [18], which showed somewhat larger scatter, seem to be slightly lower than present results too. However, all the results of the three investigations for liquid jets indicated the same trend of the shift variation of the maximum heat transfer points, although the oil jet data were determined at much lower Reynolds number than that with water jets. The maximum value of the shift measured in the three studies are quite close to each other. As shown in Fig. 4, all the maximum values are close to $0.3d$ that is significantly lower than the results report-

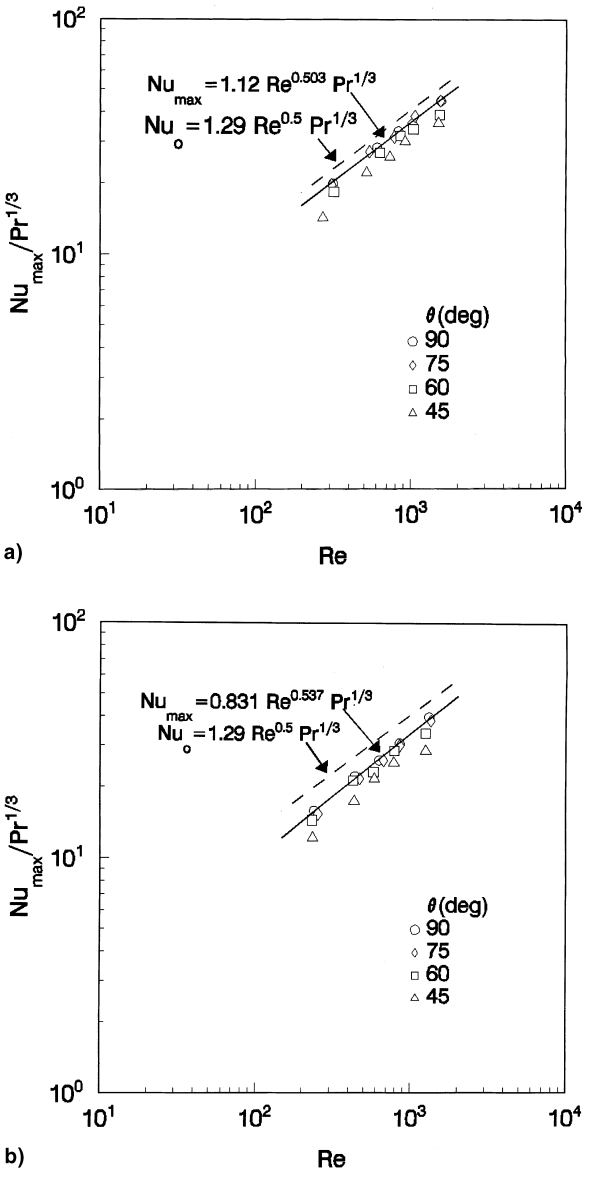

Fig. 5. Variation of maximum Nusselt number with Reynolds number at different jet inclination angles (a) Pipe-type nozzle; (b) Orifice-type nozzle.

ed with oblique air jets [16,17]. The mass transfer data reported by Sparrow and Lovell [16] for air jets are shown in the figure. Their data are higher than the liquid jet results. The data of air jets by Goldstein and Franchett [13] are even higher than those in Ref. [16]. It is noted that the Reynolds numbers both in Refs. [16,17] are higher than those in the present work, but similar to those in the study of free-surface liquid jets [18,19]. The reason is not apparent at present as to why the result of the present work is consistent with that of free-surface liquid jets [18,19] but very different from that of submerged air jets [16,17], although all the data in Refs. [16–18] were collected in the range of similar high Reynolds numbers. It is interesting to compare the present results with the displacements of the maximum pressure point with circular air jets. As shown in Fig. 4, the numerical results of Rubel [21] and the experimental results of Donaldson and Snedeker [22] and Beltaos [23] are closer to the liquid jet heat transfer data than the air jet heat transfer data while the inclination angle is greater than 50°. Similar comparison was also made in Ref. [16]. The authors found their data of maximum heat transfer displacements were much higher than those of the displacements of maximum pressure points reported by Beltaos [23]. However, the coincidence of the displacements of maximum heat transfer and pressure points has not been verified. It seems that the complexity and lack of detailed knowledge of the thermal fluid characteristics with oblique jets preclude precise statement concerning the mechanism of the displacement of the maximum heat transfer points. Further research is still required both in fluid mechanics and heat transfer.

3.2. Maximum heat transfer coefficient

Maximum heat transfer coefficient was measured with both orifice- and pipe-type nozzles over the range of jet Reynolds number from 162 to 958 at a constant nozzle-to-plate spacing of $z/d = 4$. The results are shown in Fig. 5 which demonstrate the effects of jet angle and Reynolds number on the maximum heat transfer. The maximum Nusselt number is seen in Fig. 5 to diminish with increasing of jet inclination and to increase with increasing of jet Reynolds number. An empirical formula was developed to correlate the experimental data of maximum Nusselt number

$$\mathrm{Nu}_{\max} = C\mathrm{Re}^{m}\mathrm{Pr}^{n}, \tag{5}$$

where the exponent n was set to be 1/3 [19,20] and the empirical coefficients c and m were determined using a least-squares technique to match the data obtained with pipe-type and orifice-type nozzles, respectively. The values of these coefficients and the average error of the correlation are given in Table 1 for the two types of nozzles. Eq. (5) fits all data of pipe-type and orifice-type nozzles within 5.1% and 6.9%, respectively. The predicted curves, corresponding to normal impingement ($\theta = 90°$) with the two types of nozzles respectively, are presented

Table 1
Correlation coefficients and average errors of Eq. (5)

Nozzle type	Jet angle (°)	c	m	Average error (%)
Pipe-type	90	1.11	0.503	±1.38
	75	1.05	0.512	±2.09
	60	1.11	0.491	±2.96
	45	0.708	0.543	±3.76
Orifice-type	90	0.831	0.537	±1.28
	75	0.731	0.550	±0.50
	60	0.926	0.510	±3.16
	45	0.710	0.528	±4.76

in Fig. 5. Good agreement is seen from the figure between the curves and the data. The maximum Nusselt number with orifice-type nozzle is slightly lower, about 10% than that with pipe-type. It is important to note that the Reynolds number dependence of maximum Nusselt number is characterized with a power function about 0.5. This exponent value clearly indicates the laminar characteristic of oblique jet flow in stagnation zone. Also present in the figures is the correlation by the present authors based on pipe nozzle data [6,20]

$$\mathrm{Nu}_0 = 1.29\ \mathrm{Re}^{0.5}\mathrm{Pr}^{1/3}. \quad (6)$$

Agreement is expectantly observed between the correlation and the pipe nozzle data in this study. The Nusselt number obtained from orifice nozzle is lower than that associated with pipe nozzle as shown in Fig. 5.

It can be seen from Fig. 5 and Table 1 that there is a clear trend for the maximum Nusselt number to diminish with increasing jet inclination as reported previously with air jets [15,16]. As shown in the table and the figure with moderate jet inclination, the decrease in peak heat transfer is obviously apparent. However, over a small range of jet inclination close to normal direction to the target surface, the maximum Nusselt number is insensitive with the change in jet angle. The maximum Nusselt number decreases monotonically with farther increasing of the jet inclination. In the present study the decreases of the maximum Nusselt number with jet inclination were 15.9% and 19.7% at jet angle of 45°, respectively for pipe-type and orifice-type nozzles. This result is slightly higher than with that recorded with circular air jets. At the same jet angle (45°), decreases in maximum heat transfer were reported to be 14% and 11% by Sparrow and Lovell [16] and Goldstein and Franchett [17], respectively.

3.3. Local heat transfer coefficient profiles

The main body of the present work is measured profiles of local Nusselt number at representative values of Reynolds number and jet inclination. The local heat transfer were measured and plotted as a function of radial position along two principal axes of the wall jets: horizontal (x) and vertical (y) axes, with origin situated at the point of maximum heat transfer for each specific case. Measurements were made both for pipe-type and orifice-type nozzles. The results of pipe-type nozzle are presented for various jet angles (90°, 75°, 60°, 45°) in Figs. 6–8. On the abscissa the radial distances are measured in terms of the jet nozzle diameter, while on the ordinates local Nusselt numbers are presented after normalization to the maximum Nusselt number for each case.

Considering first the heat transfer distribution for pipe nozzle in y-axis, it may be seen from Fig. 6 that all the y-axis profiles at various jet angles generally display the bell shape. As shown in the figures, all these profiles are essentially symmetric about the maximum heat transfer point for each case. If comparisons are made from figure to figure, it can be found that the local

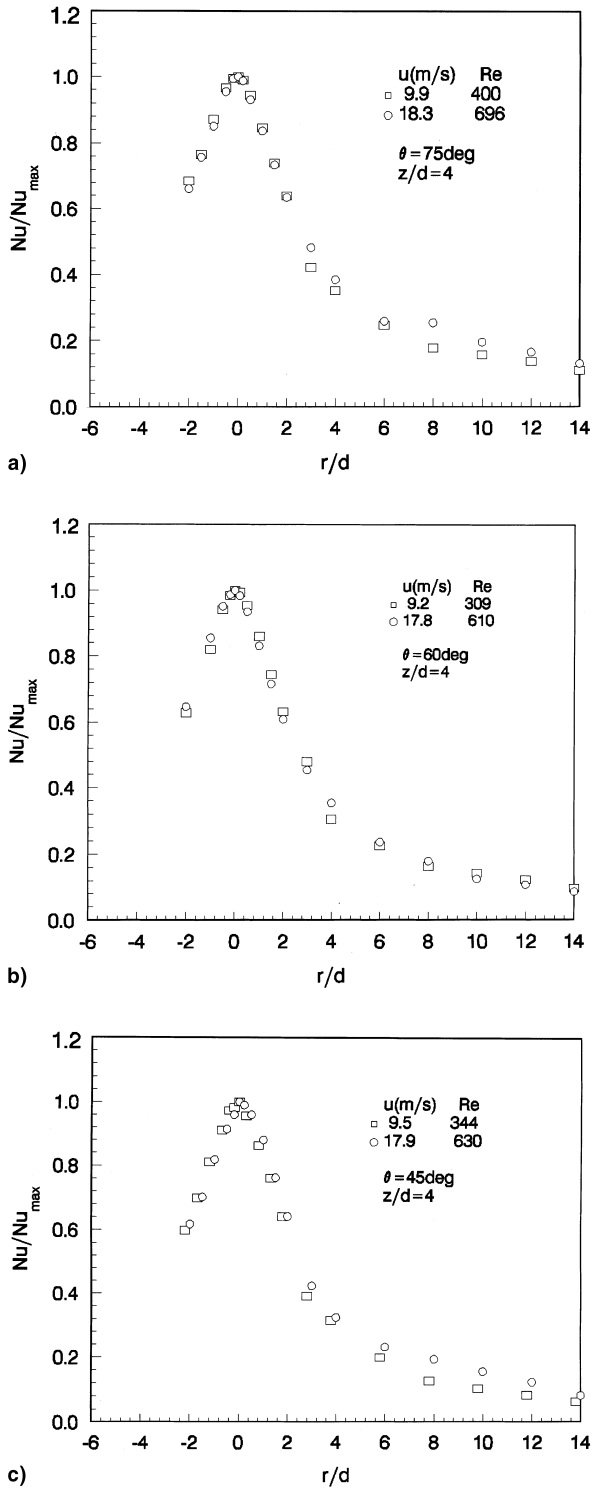

Fig. 6. Local Nusselt number distributions along y-axis (pipe-type nozzles) (a) $\theta = 75°$; (b) $\theta = 60°$; (c) $\theta = 45°$.

distributions in y-axis are insensitive with jet inclination in the ranges of the parameters encountered in this study. Actually, the profiles seem to be not affected by the variation of jet inclination. This tendency was also reported by Sparrow and Lovell [16] with circular obli-

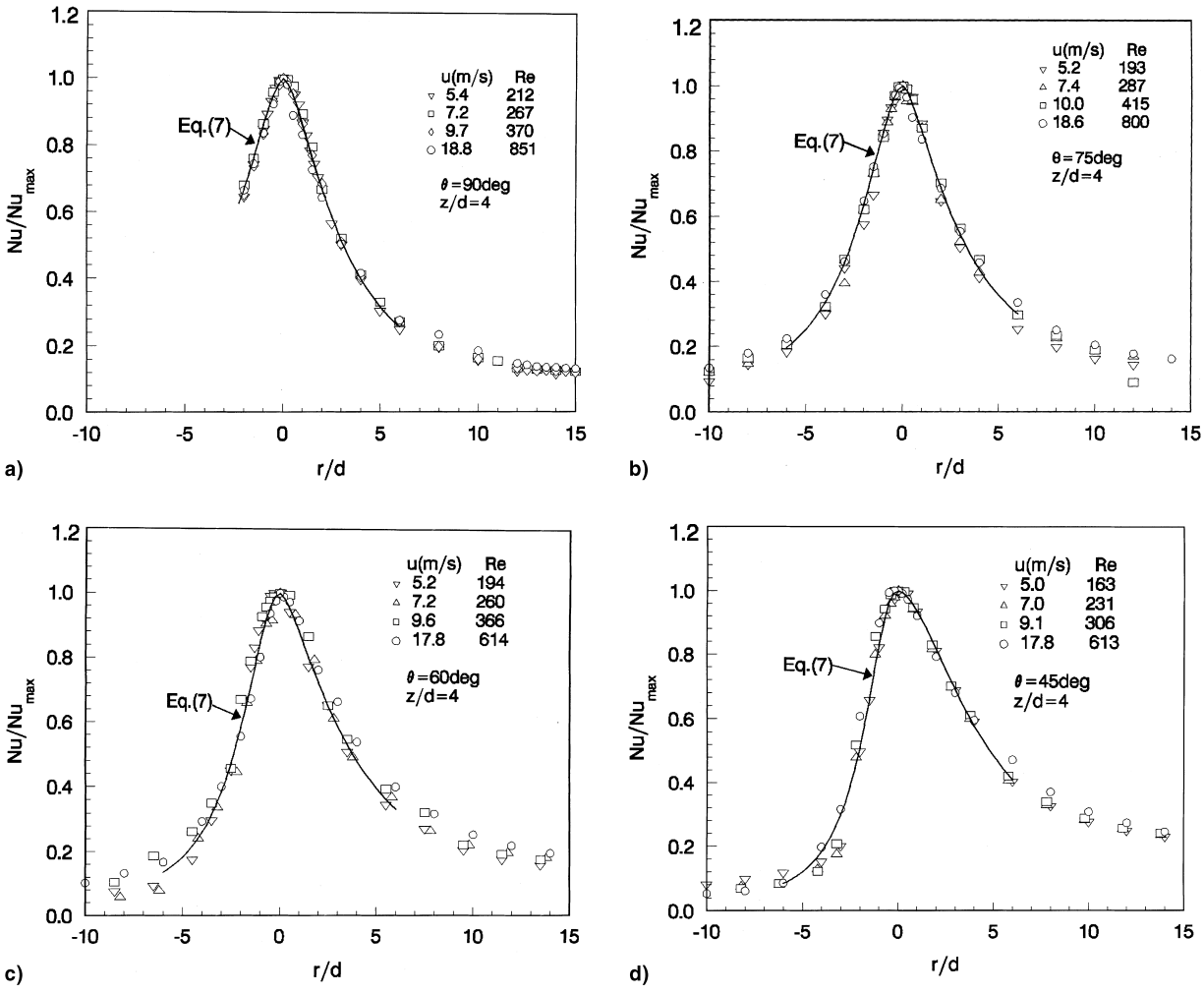

Fig. 7. Local Nusselt number distributions along x-axis (pipe-type nozzles) (a) $\theta = 90°$; (b) $\theta = 75°$; (c) $\theta = 60°$; (d) $\theta = 45°$.

que air jets. The Reynolds number dependence of local heat transfer profiles along y-axis can be also observed in Fig. 6 which indicates that the profiles are essentially independent of Reynolds number.

With regard to the local heat transfer profiles along the x-axis, the experimental results shown in Figs. 7 and 8, for the pipe and orifice nozzles respectively, exhibit more complicated characteristics of convective heat transfer. For normal impingement ($\theta = 90°$), symmetric bell shape is seen of the profiles in the figures. For oblique impingement, although a general bell-shape is also observed for the profiles, the distribution curves are not symmetric about the maximum heat transfer point. The heat transfer coefficient on the downstream side is higher than that in the upstream side. This asymmetry is the most prominent feature of oblique jet impingement heat transfer, and has been reported both with circular air jets [16,17] and free-surface liquid jets [18,19]. The shape of the asymmetric distribution curves of local heat transfer in x-axis was significantly affected by the jet inclination. By comparing the profiles for various jet angles in Figs. 7 and 8, the asymmetry in the profiles in the present study is seen to be accentuated at smaller jet angles. The values of heat transfer coefficient on the downstream side increased while that on the upstream side decreased as increasing the jet inclination. The decrease in jet angles caused increase in slope of the profile curves on upstream side and decrease in the slope on the other side. Consequently, a more significant imbalance may be caused by increasing jet inclination in the heat transfer capabilities on the two sides. The influence of Reynolds number can also be examined in the figures. It is seen from the figures that all the curves for different values of Reynolds number tend to collapse to a single profile for each inclination angle after normalization to the maximum Nusselt number in the stagnation zone ($r/d < 2$). It means that local Nusselt number profiles are independent of Reynolds number when divided by the Reynolds number raised to the power of 0.503 and 0.537 for pipe and orifice nozzles, respectively. Similar tendency was also reported for circular air jets [16,17] and free-surface liquid jets [18,19]. In the wall jet zone ($r/d > 2$), the profiles seem to be very slightly influenced by Reynolds number. As shown in

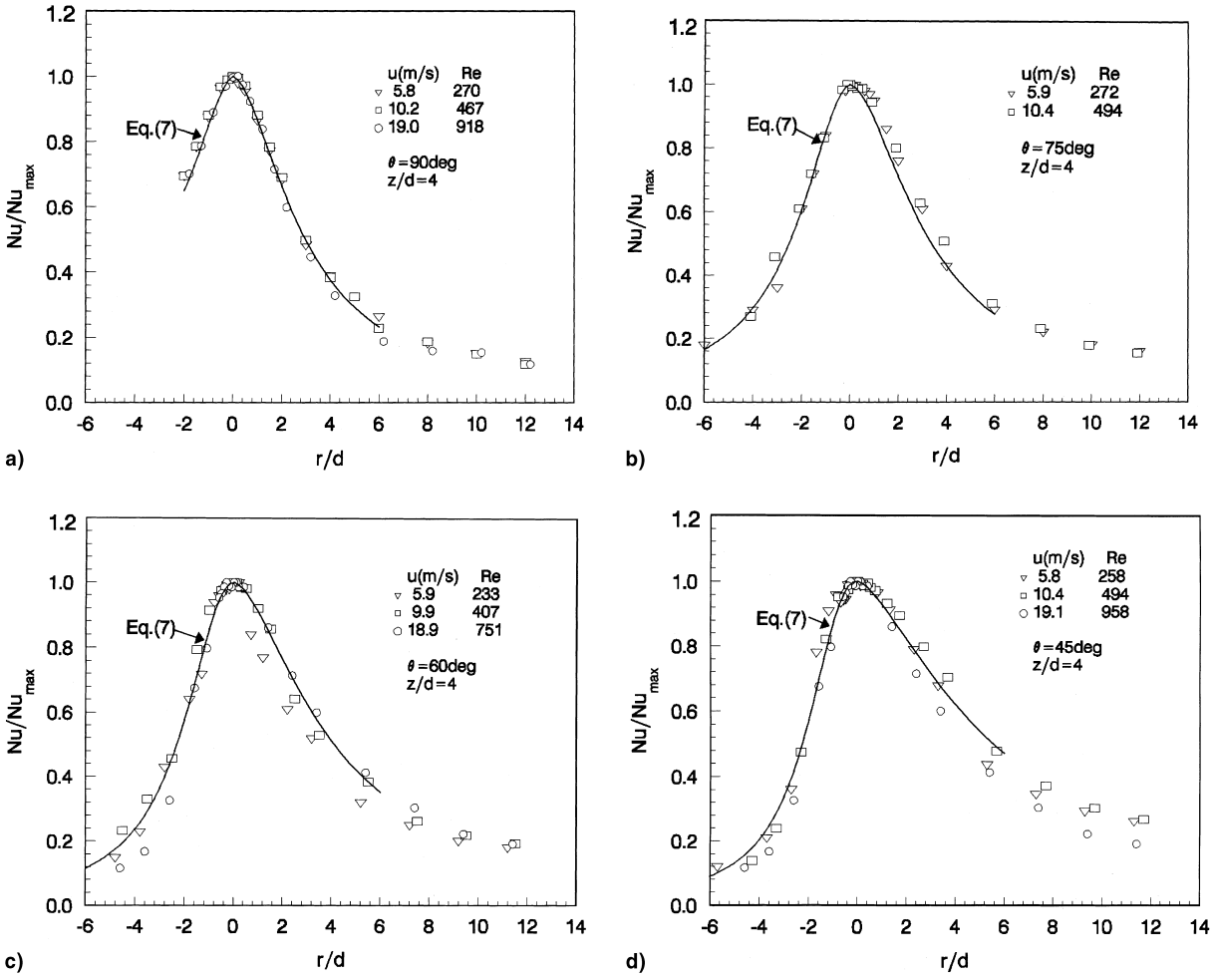

Fig. 8. Local Nusselt number distributions along x-axis (orifice-type nozzle) (a) $\theta = 90°$; (b) $\theta = 75°$; (c) $\theta = 60°$; (d) $\theta = 45°$.

the figures it appears that the profiles of larger Reynolds number decline a little bit more slowly than those of smaller Reynolds number. To a first approximation, the effect of Reynolds number can be neglected. It is noted that the profiles from the two types of nozzles are very similar with each other. An empirical equation was developed to correlate all the local heat transfer data along the x-axis within $|r/d| \leqslant 6$:

$$\mathrm{Nu} = \frac{\mathrm{Nu}_{\max}}{1 + A(r/d)^P}, \tag{7}$$

where

$$A = A_0 + A_1 \sin\theta + A_2 \sin^2\theta,$$

$$P = P_0 + P_1\theta + P_2\theta^2.$$

The values of the coefficients in Eq. (7) were determined from least-squares fits of the experimental data for pipe-type and orifice-type nozzles, respectively. They are given in Table 2. $\mathrm{Nu}_{\max}$ in Eq. (7) can be calculated from Eq. (5) with the constants given in Table 1.

Eq. (7) fits 88% and 73% of the data with pipe-type and orifice-type nozzles, respectively, within ±10% for all the measured Reynolds numbers and jet angles.

Table 2
Empirical constants in Eq. (7)

Nozzle type	Location	A_0	A_1	A_2	P_0	P_1	P_2
Pipe-type	$r/d > 0$	0.372	−0.281	0.0929	2.96	−1.05	−0.124
	$r/d < 0$	−0.331	0.707	−0.252	3.18	−2.79	1.14
Orifice-type	$r/d > 0$	−0.0122	0.270	−0.0942	3.11	−0.863	−0.0686
	$r/d < 0$	0.0472	0.00590	0.0406	0.617	1.55	−0.551

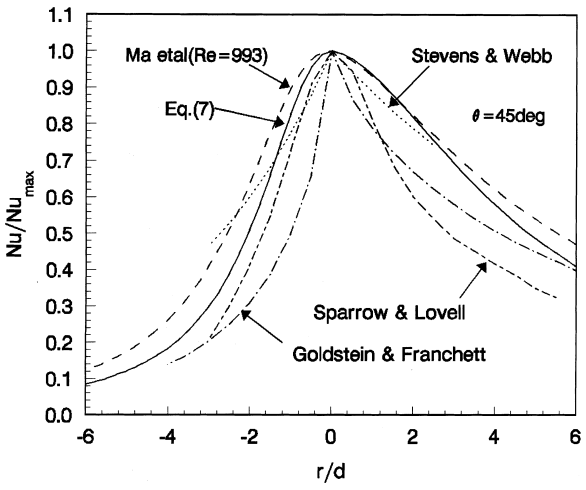

Fig. 9. Comparison of x-axis Nusselt number profiles between oblique circular liquid and air jets ($\theta = 45°$).

Comparison is made between the correlation and the experimental data both from the two nozzles in Figs. 7 and 8. In general, good agreement is observed from the figures.

Finally, comparison is made between the present results and previous works with oblique impinging jets. At a jet inclination angle of 45°, the present correlation Eq. (7) is displayed in Fig. 9 together with those by Goldstein and Franchett [17] for circular air jets and by Stevens and Webb [18] and Ma et al. [19] for circular free-surface jets of water and transformer oil, respectively. Experimental data reported by Sparrow and Lovell [16] are also presented in the figure for comparison. All the correlations and data in the figure indicate a general trend of the local characteristics of oblique impingement heat transfer along the x-axis. Considering the differences in the test fluids, jet velocities, nozzle geometry and jet operation modes, some disagreements observed in Fig. 9 between the five investigations would be quite understandable.

4. Conclusions

1. Experimental study was conducted to measure and to characterize the local convective heat transfer from vertical heaters to obliquely impinging circular submerged jets of transformer oil. The measurements were made with both pipe-type and orifice-type nozzles in the range of Reynolds number from 162 to 958.
2. Displacement of maximum heat transfer points was observed and measured with jet inclination angles from 90° to 45°. All the experimental data of the displacement can be correlated by Eq. (4). It seems that displacement measured with submerged oil jets is slightly larger than that with free-surface oil jets.
3. Maximum heat transfer coefficients were measured and found to be decreased with increasing of jet inclination. The data of maximum Nusselt number can be well correlated with Eq. (5). The measured maximum Nusselt numbers with the pipe-type nozzle are slightly higher than those measured with the orifice-type nozzle.
4. Local heat transfer profiles were measured along both x and y-axes. The x-axis profiles exhibit an increasing asymmetry with increasing of jet inclination. All the data of local Nusselt number along the x-axis can be correlated by Eq. (7). The y-axis profiles are essentially independent of the variation of the jets inclination. After normalization to maximum Nusselt number, local heat transfer profiles in both x and y-axes are insensitive with Reynolds number in the present study.

Nomenclature

A	area of heated surface, empirical constants
c	empirical constant
C_p	specific heat at constant pressure
d	jet nozzle diameter
h	local heat transfer coefficient
I	current intensity
k	thermal conductivity of fluid
m,n	empirical constants
Nu	local Nusselt number, hd/k
P	empirical constants
Pr	Prandtl number, $C_p\mu/k$
q	heat flux
R	electrical resistance
r	radial distance from stagnation point, recovery factor
Re	Reynolds number, ud/v
s	displacement of the maximum heat transfer point from the geometric stagnation point
T_{aw}	adiabatic wall temperature
T_j	jet static temperature at nozzle exit
T_w	wall temperature
u	mean fluid velocity at nozzle exit
z	nozzle-to-plate spacing

Greek symbols

θ	jet inclination angle
μ	dynamic viscosity
v	kinematic viscosity

Subscripts

max	maximum value
o	normal impingement ($\theta = 90°$)

Acknowledgements

This work was supported by the National Natural Science Foundation of China. The authors are indebted to Mr. D.H. Lei for help in the experiments, and to Profs. S.Y. Ko at Chinese Academy of Science and B.W. Webb at Brigham Yong University for their valuable suggestions.

References

[1] H. Martin, Heat and mass transfer between impinging gas jets and solid surfaces, Advances in Heat Transfer 13 (1977) 1–60.

[2] H.T. Downs, E.H. James, Jet impingement heat transfer – A literature survey, ASME Paper, 87-HT-35, 1987.

[3] P. Hrycak, Heat transfer from impinging jets – A literature review, Technical Report AFWAL-TR-81-3504, Flight Dynamics Laboratory, Wringht Patterson AFB, Ohio, 1981.

[4] B.W. Webb, C.F. Ma, Single-phase liquid jet impingement heat transfer, Advances in Heat Transfer 26 (1995) 105–217.

[5] C.F. Ma, Liquid jet impingement heat transfer with or without boiling, in: Proceedings of the 10th National Heat Transfer Congress, Genova, Italy, 25–27 June 1992, pp. 35–60. Also in J. Thermal science 5 (2) (1993) 128–131.

[6] M. Kiryu, Development of oil-cooled 750 cc motorcycle engine, Automobile Technology (in Japanese) 40 (1986) 1154–1158.

[7] H. Sun, C.F. Ma, W. Nakayama, Local characteristics of convective heat transfer from simulated microelectronic chips to impinging submerged round water jets, ASME J. Electronic Packaging 115 (1993) 71–77.

[8] L.M. Jiji, Z. Dagan, Experimental investigation of single phase multi-jet impingement cooling of an array of microelectronic heat sources, in: Win Aung (Ed.), Cooling Technology for Electronic Equipment, Hemisphere, Washington, DC, 1988, pp. 333–352.

[9] D.C. Wadsworth, I. Mudawar, Cooling of multichip electronic module by means of confined two-dimensional jets of dielectric liquid, ASME J. Heat Transfer 112 (1990) 891–898.

[10] D.J. Womac, S. Ramadhyani, F.P. Incropera, Correlating Equations for Impingement Cooling of Small Heat Surfaces with Single Circular Liquid Jets, ASME Journal of Heat Transfer 115 (1993) 106–115.

[11] D.E. Maddox, A. Bar-Cohen, Thermofluid design of submerged jets impingement cooling for electronic components, ASME HTD 171 (1991) 71–80.

[12] C.F. Ma, A.E. Bergles, Boiling jet impingement cooling of simulated microelectronic chips, ASME HTD 28 (1983) 5–12.

[13] F.C. Kohing, Waterwall: Water cooling systems, Iron-Steel Engineer 62 (1985) 30–36.

[14] C.F. Ma, J. Yu, D.H. Lei, Y.P. Gan, F.K. Tsou, H. Auracher, Transient jet boiling heat transfer on hot surfaces, in: X.J. Chen et al. (Ed.), Multiphase Flow and Heat Transfer – Second International Symposium, vol. 1, Hemisphere, Washington, DC, 1990, pp. 349–357.

[15] K.P. Perry, Heat transfer by convection from a hot gas jet to a plane surface, Proceedings of the Inst. Mech. Eng. 168 (1954) 775–780.

[16] E. Sparrow, B.J. Lovell, Heat transfer characteristics of an obliquely impinging circular jet, ASME J. Heat Transfer 102 (1980) 202–207.

[17] R.J. Goldstein, M.E. Franchett, Heat transfer from a flat surface to an oblique impinging jet, ASME J. Heat Transfer 110 (1988) 84–90.

[18] J. Stevens, B.W. Webb, The effect of inclination on local heat transfer under an axisymmetric free liquid jet, Int. J. Heat Mass Transfer 34 (1991) 1227–1236.

[19] C.F. Ma, Q. Zheng, H. Sun, K. Wu, T. Gomi, B.W. Webb, Local characteristics of impingement heat transfer with oblique round free-surface jets of large prandtl number liquid, Int. J. Heat Mass Transfer 40 (10) (1997) 224–2259.

[20] C.F. Ma, H. Sun, H. Auracher, T. Gomi, Local convective heat transfer from vertical heated surfaces to impinging circular jets of large prandtl number liquid, Proceedings of the Ninth International Heat Transfer Conference 2 (1990) 441–446.

[21] A. Rubel, Oblique impingement of a round jet on a plane surface, AIAA J. 20 (1982) 1756–1758.

[22] C.D. Donaldson, R.S. Snedeker, A study of free jet impingement, Part 1: Mean properties of free and impinging jets, J. Fluid Mech. 45 (1971) 281–319.

[23] S. Beltaos, Oblique impingement of circular turbulent jets, J. Hydraulic Res. 14 (1976) 17–36.